Biochemistry and Biophysics Reports 18 (2019) 100621

Contents lists available at ScienceDirect

Biochemistry and Biophysics Reports

journal homepage: www.elsevier.com/locate/bbrep

# A cell-based high-throughput screen identifies tyrphostin AG 879 as an inhibitor of animal cell phospholipid and fatty acid biosynthesis

Raphael A. Zoeller*, Kathleen Geoghegan-Barek

*Department of Physiology & Biophysics, Boston University School of Medicine, 700 Albany Street, Room W302, Boston, MA, 02118, USA*

ARTICLE INFO

*Keywords:*
Phospholipid biosynthesis
Fatty acid biosynthesis
Tyrphostin AG 879
Antiviral
Anticancer
Drug screening

ABSTRACT

Inhibition of animal cell phospholipid biosynthesis has been proposed for anticancer and antiviral therapies. Using CHO−K1 derived cell lines, we have developed and used a cell-based high-throughput procedure to screen a 1280 compound, small molecule library for inhibitors of phospholipid biosynthesis. We identified tyrphostin AG 879 (AG879), which inhibited phospholipid biosynthesis by 85–90% at a concentration of 10 μM, displaying an $IC_{50}$ of 1–3 μM. The synthesis of all phospholipid head group classes was heavily affected. Fatty acid biosynthesis was also dramatically inhibited (90%). AG879 inhibited phospholipid biosynthesis in all additional cell lines tested, including MDCK, HUH7, Vero, and HeLa cell lines. In CHO cells, AG879 was cytostatic; cells survived for at least four days during exposure and were able to divide following its removal. AG879 is an inhibitor of receptor tyrosine kinases (RTK) and inhibitors of signaling pathways known to be activated by RTK's also inhibited phospholipid biosynthesis. We speculate that inhibition of RTK by AG879 results in an inhibition of fatty acid biosynthesis with a resulting decrease in phospholipid biosynthesis and that AG879's effect on fatty acid synthesis and/or phospholipid biosynthesis may contribute to its known capacity as an effective antiviral/anticancer agent.

## 1. Introduction

All living organisms produce phospholipids, required for the formation of membranes. Animal cells tightly regulate the rate of phospholipid production, with quiescent cells synthesizing phospholipids at a relatively slow pace and rapidly dividing cells producing phospholipids at an enhanced rate [1,2]. While the enzymology involved in producing phospholipids in animal cells has been fairly well described [2], the mechanism(s) behind regulation, as well as dysregulation, of phospholipid biosynthesis is only beginning to emerge.

Rapidly dividing cells, such as cancer cells, require a constant supply of phospholipids. Inhibition of phospholipid biosynthesis has therefore been proposed as an attractive target for anticancer therapies [1]. Variant animal cell lines, defective in phospholipid biosynthesis display dramatically slower growth rates [3–6]. Also, inhibitors of phospholipid biosynthesis have been shown to inhibit cancer cell growth in culture [7–9]. Similarly, viral replication in animal cells has been shown to stimulate phospholipid synthesis [10–13] while inhibition of phospholipid biosynthesis inhibits viral replication in animal cells [10] and yeast [14]. Development of animal cell phospholipid biosynthesis inhibitors is therefore an attractive avenue for both anticancer and antiviral protocols.

There are relatively few available inhibitors of phospholipid biosynthesis. Bromoenol lactone is a suicide inhibitor of phosphatidate phosphohydrolase, effective in the range of 30 μM [9,15]; it also inhibits calcium independent phospholipase $A_2$ at lower concentrations [16]. Propanolol has also been shown to inhibit phospholipid biosynthesis in the range of 50–200 μM [9]. Inhibitors of phosphatidylcholine biosynthesis have been identified and are effective in inhibiting cancer cell growth in culture [7,8,17,18].

Additional inhibitors would greatly aid in the development of anticancer/antiviral treatments. The lack of available phospholipid biosynthesis inhibitors has been a consequence of a lack in high-throughput protocols to screen small molecule libraries for phospholipid biosynthesis inhibitors. Here we report the development and use of cell-based high-throughput screen to identify a compound, AG879,

*Abbreviations:* RTK, Receptor tyrosine kinase; $^{32}P_i$, [$^{32}$P]orthophosphate; P12, 12-(1′-pyrene) dodecanoic acid; AG879, Tyrphostin AG 879; HTS, High-throughput screen; EGFR, Epidermal growth factor receptor; trkA, Tropomyosin analogue receptor kinase; HER2, Human epidermal growth factor receptor 2; AFU, Arbitrary fluorescence units; PL, Phospholipid; PC, Phosphatidylcholine; PE, Phosphatidylethanolamine; PI, Phosphatidylinositol; PA, Phosphatidic acid; CL, Cardiolipin; TG, Triacylglycerol; CE, Cholesterol ester

* Corresponding author.
*E-mail address:* rzoeller@bu.edu (R.A. Zoeller).

https://doi.org/10.1016/j.bbrep.2019.100621
Received 11 January 2019; Accepted 18 February 2019
Available online 06 March 2019

which is effective in inhibiting animal cell phospholipid biosynthesis, is non-toxic in the short-term (up to 4 days in culture) and has previously been reported to be an effective anticancer and antiviral compound.

## 2. Materials and methods

### 2.1. Materials

[$^{32}$P]inorganic phosphate ($^{32}P_i$; 9,000 Ci/mmol), [9,10-$^{3}$H]palmitic acid (43 Ci/mmole), [1–$^{14}$C]oleic acid (54.6 mCi/mmol), and [$^{3}$H] acetic acid (100 mCi/mmol) and [methyl-$^{14}$C]choline (50 mCi/mmol) were obtained from Perkin Elmer (Boston, MA). Lipid standards were purchased from Avanti Polar Lipids. Silica gel G and silica gel 60 thin-layer chromatography plates (EMD), Ham's F12 and DMEM medium (Cellgro or Gibco), fetal bovine serum (HyClone) and tissue culture dishes were obtained from ThermoFisher Scientific. All other reagents, unless otherwise specified, were purchased from Aldrich/Sigma.

### 2.2. Cell lines and cell culture conditions

The ZR-82 cell line is a peroxisome-deficient variant of the wild-type CHO−K1 cell line [19]. The GroD1 cell line is a variant of ZR-82 which is 85% deficient in phospholipid biosynthesis [20]; GroD1 cells are able to grow at 33°C (albeit somewhat more slowly than ZR-82 cell), more slowly at 37°C, but they do not grow 40°C. CHO−K1 based cell lines were maintained in Ham's F12 medium supplemented with 10% fetal bovine serum, 1 mM glutamine, penicillin G (100 U/ml) and streptomycin (75 U/ml) using 5% $CO_2$. All other cells were maintained in, and experiments were performed in, DMEM supplemented with 10% fetal bovine serum, 1 mM glutamine, penicillin G (100 U/ml) and streptomycin (75 U/ml).

### 2.3. Cell-based high-throughput screen for phospholipid biosynthesis inhibitors

Cells were plated into 384-well plates at $1.25 \times 10^3$ cells/well in 30 μl medium and allowed to attach overnight @ 33°C, the permissive temperature for growth of the GroD1 cells. Cells were shifted to 37°C for 3 h and 10 μl growth medium containing 70 μM test compound followed by the addition of 30 μl growth medium containing 47 μM 1-*O*-[12-(1′-pyrene)]dodecanoic acid (P12) were added to achieve a final concentration of 20 μM P12 and 10 μM test compound (with a 0.1% DMSO concentration). After 3 h at 37°C, the medium containing P12 and any test compound was removed and 70 μl of fresh medium was added to sequester any remaining P12 that was not incorporated into complex lipids in the cells. After 30 min @ 37°C, cell monolayers were placed on a 1.5 mm thick borosilicate glass plate suspended over two 15 W long-wavelength (> 300 nm) UV bulbs in a Black-Ray UV lamp (Model XX-15L, UVP, Inc., San Gabriel, CA) and irradiated from underneath for 2–5 min at an intensity of 1200 μW/cm$^2$, measured at 365 nm using a J-series UVP, Inc. Ultraviolet meter. Cell viability was measured after 24 h growth at 33°C by adding 14 μl CellTiter Blue® (Promega, USA) and fluorescence was read after 3 h at 33C using a TECAN plate reader (560 nm Ex/590 nm Em). Negative wells had vehicle (0.1% DMSO) added to ZR-82 cells instead of compounds while positive wells contained the phospholipid biosynthesis-deficient variant, GroD1 with 0.1% DMSO added. All candidate compound tests used wells contained ZR-82 cells. Fig. 1 graphically outlines the steps involved in the screening protocol.

### 2.4. Phospholipid biosynthesis

For phospholipid biosynthesis, short-term labeling with $^{32}P_i$ or [methyl-$^{14}$C]choline was used. Cells were plated into six-well tissue culture plates ($2.5 \times 10^5$ cells/well) and allowed to attach overnight. The next day medium was changed to 1 ml of growth medium containing $^{32}P_i$ (20–50 μCi/ml) or [methyl-$^{14}$C]choline (5 μCi/ml) and incubated for 3 h at 37°C. Medium was removed, the cell monolayer was washed once with 2 ml PBS, phospholipids were then recovered with 2 ml methanol containing 500 μg carrier lipid (total bovine heart extract) and extracted according to the method of Bligh and Dyer [21]. After extraction, solvent was removed by evaporation under a $N_2$ stream and the dried lipids were re-suspended in $CHCl_3$. An aliquot was taken to determine total $CHCl_3$-soluble radioactivity. $^{32}P_i$-labeled phospholipids were separated by two-dimensional thin-layer chromatography (2D TLC) using silica gel 60 plates as described [20]. Individual phospholipid species were located by autoradiography and co-migration with authentic standards. Bands were scraped and radioactivity was quantitated using liquid scintillation spectrometry. [Methyl-$^{14}$C]choline-labeled phospholipids were not separated into individual species using TLC.

When the effects of fatty acid supplementation on phospholipid biosynthesis was examined, stock solution (in ethanol) of oleic acid was added to growth medium contained in a sterile glass scintillation vial. The medium was mixed then sonicated in a water bath for 10 min. After incubation at 37°C for 60 min, $^{32}P_i$ was added to media and phospholipid biosynthesis was measure as described above.

### 2.5. Fatty acid biosynthesis

Fatty acid biosynthesis was measured using [$^{3}$H]acetate. Cells ($5 \times 10^5$ cells/vial) were plated into sterile glass scintillation vials in 3 ml medium and allowed to attach overnight. Growth medium was changed the following day. Approximately 48 h after plating, medium was removed and replaced with 1 ml medium containing 50 μCi [$^{3}$H] acetate/ml. After 3 h at 37°C, labeling medium was removed, and the cell monolayers were washed using 3 ml PBS. PBS was removed and 3.8 ml of a single phase Bligh & Dyer mixture [21] of $CHCl_3$:$CH_3OH$:PBS (1:2:0.8; v:v) containing 500 μg total bovine liver lipids as carrier was added to extract labeled cellular lipids. 1 ml $CHCl_3$ and 1 ml PBS were then added and vortexed to form a two-phase mixture and this was centrifuged at 600 × *g* for 5 min to separate phases. The lower, organic phase was recovered, the upper, aqueous phase was washed once with 2 ml $CHCl_3$ and the two organic extracts were combined. Solvent was evaporated under a stream of $N_2$ and the lipids were incubated in 0.5 ml 1 N NaOH in 90% ethanol for 1 h at 80°C to generate unesterified fatty acids (free fatty acids). After addition of 1 ml 1.5 N HCl, the free fatty acids were extracted twice with 3 ml hexane. Combined hexane extracts were blown to dryness and re-suspended in $CHCl_3$, spotted on a silica gel G TLC plate and fatty acids were purified using hexane: ethyl ether: acetic acid (75:25:1; v:v). Bands corresponding to free fatty acids were identified by co-migration with authentic standards following iodine vapor staining [22], and these were scraped from the TLC plate and radioactivity was determined using liquid scintillation spectrometry.

### 2.6. Fatty acid uptake and distribution

For P12 uptake, cells were plated into 96-well plates at $2 \times 10^4$ cells/well and allowed to attach overnight. Medium was removed and replaced with medium containing 20 μM P12 and the indicated concentration of AG879. After 3 h at 37°C, this medium was removed and replaced with 120 μl fresh medium. After 30 min at 37°C, medium was removed and replaced with 100 μl RIPA buffer. After mixing for 30 min on a rotation table, fluorescence was read using a TECAN plate reader (340 nm Ex/378 nm Em).

For palmitic acid uptake, cells ($5 \times 10^5$ cells/vial) were plated into sterile glass scintillation vials in 3 ml medium and allowed to attach overnight. Medium was removed and cells were incubated in 1 ml medium containing 20 μM [9,10-$^{3}$H]palmitic acid for 3 h. Medium was removed, and the cell monolayer was incubated for 30 min in 2 ml fresh growth medium. Following a wash with 3 ml PBS, the cellular lipids were extracted directly from vials according to the method of Bligh and

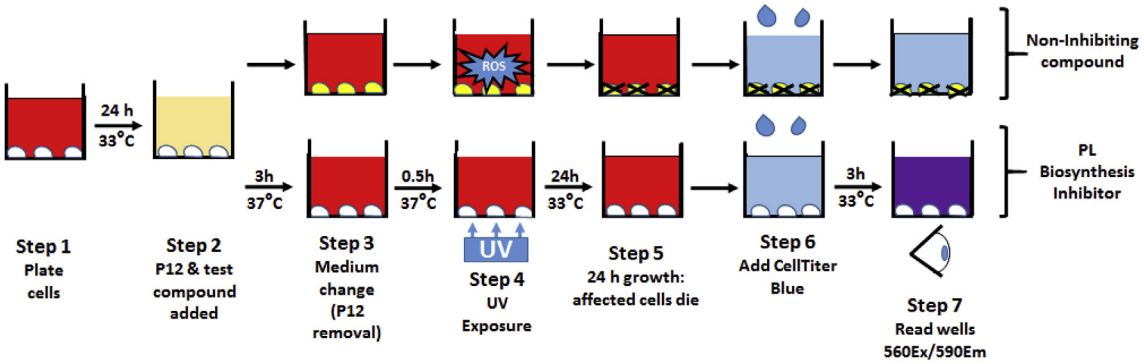


**Fig. 1. Steps involve the cell-based HTS. Step 1:** Cells are plated out and allowed to form monolayers at 33°C for 24 h. **Step 2:** Medium containing P12 and a test compound is added to achieve a final concentration of 20 μM P12 and 10 μM test compound. **Step 3**: After 3 h at 37°C, medium is removed and replaced with normal growth medium to remove any P12 not incorporated into complex lipids. **Step 4:** Irradiate cells with long wavelength UV light from underneath to generate cytotoxic ROS in P12-containing cells. **Step 5:** Incubate at 33°C for 24 h to allow surviving cells to grow while affected cells die. **Step 6:** CellTiter Blue is added. **Step 7:** After a 3 h incubation at 33°C, fluorescence generated from CellTiter Blue by surviving cells is measured.
**Non-Inhibiting Compound:** Compound does not inhibit PL biosynthesis, P12 accumulates and cells are killed upon UV exposure. **PL Biosynthesis Inhibitor:** PL biosynthesis is inhibited, cells accumulate less P12, less ROS is generated, and cells survive.

Dyer [21] and separated using single dimension TLC on silica gel G plates using hexane: ethyl ether: acetic acid (70:30:1; v/v) as the development system. Bands of interest, based on co-migration with authentic standards, were scraped from the plate and radioactivity quantitated using liquid scintillation spectrometry.

### 2.7. Triglyceride and cholesterol ester accumulation

ZR-82 cells were plated in 100 mm diameter tissue culture dishes at $2 \times 10^6$ cells/dish and allowed to attach overnight at 37°C. The next morning, the medium was changed to Ham's F12 media containing 10% FBS and 200 μM oleic acid with or without AG879. Cells were grown at 37°C for 24 h after which they were harvested with trypsin, cell counts were taken, and lipids were extracted as described above. Lipids were separated using single dimension TLC on silica gel G plates using hexane: ethyl ether: acetic acid (70:30:1; v/v) as the development system. Neutral lipid species were visualized by heating the TLC plate after spraying it with 50% sulfuric acid to char the lipids.

### 2.8. Colony formation

Cell survival was visualized by staining colonies, generated from surviving cells, following AG879 treatment. ZR-82 cells were plated at low density (100 cells/dish) in 60 mm diameter dishes in 2 ml medium and allowed to attach overnight. Medium containing AG879 or DMSO was added to achieve a final concentration of 10 μM AG879 and 0.1% DMSO. DMSO-treated cells were allowed to grow for 10 days prior to staining with Coomassie blue. AG879-treated cells were maintained in the presence of the compound for 4 days, the medium was then changed to AG879-free medium. Colonies resulting from surviving cells were stained after an additional 10 days of growth. For staining colonies, medium was removed, cells were rinsed twice with PBS, then stained with 0.5% Coomassie blue in methanol:water:acetic acid (45:45:10; v/v) for 30 min, followed by three washes of 10 min each with methanol:water:acetic acid (45:45:10; v/v). Stained colonies were allowed to dry prior to digitization of the plates using a commercial desktop scanner.

### 2.9. Measurement of cellular ATP levels

Cellular ATP levels were measured using the ENLITEN® luciferase bioluminescent kit assay (Promega, Madison, WI) following the manufacturer's protocol. ATP was extracted in 0.5% trichloroacetic acid, and aliquots were used for ATP determination using luminescence measured using a TECAN multiplate reader.

### 2.10. Statistical analysis

A two-tailed Student's t-test was used. All values represented the average ± standard deviation (SD). Values of $p \leq 0.05$ were considered significant differences and annotated using *.

## 3. Results

### 3.1. High-throughput screen discovers a phospholipid biosynthesis inhibitor

Previously, we reported the use of a fluorescent fatty acid, P12, to select for Chinese hamster ovary (CHO) variant strains which were defective in phospholipid biosynthesis [20]. This selection was based on the hypothesis that cells less able to synthesize phospholipids would accumulate less P12 when incubated in medium containing this fluorescent fatty acid. With reduced P12, these cells would be less sensitive to the cytotoxic effects of long wavelength (> 300 nm) ultraviolet irradiation, which excites the pyrene moiety, resulting in the generation of cytotoxic reactive oxygen. This is demonstrated by the reduced sensitivity of the phospholipid biosynthesis-deficient cell line, GroD1 [20], compared to phospholipid biosynthesis-competent parent strain, ZR-82 [19], to a 3 h exposure to medium containing P12, followed by exposure to UV light (Fig. 2). The GroD1 cell line displays a severe reduction in phosphatidate phosphohydrolase activity [23], resulting in reduced synthesis of all glycerolipids which are dependent upon this activity [20]. These include phosphatidylcholine (PC), phosphatidylethanolamine (PE), and triacylglycerol (TG).

With no UV irradiation, the values for GroD1, when measuring viable cell numbers using CellTiter Blue, were reduced compared to ZR-82. This is due to the slower growth of this latter cell line over the two day period required for the screening protocol. However, ZR-82 cells were more affected by UV irradiation following exposure to P12; after exposure to UV light for 4–5 min, the signal from the phospholipid biosynthesis-competent ZR-82 cells was comparable to no-cell control wells while there was still significant signal from the GroD1 cells.

We adapted this protocol for use in a cell-based high throughput screen (HTS) for small molecule inhibitors of phospholipid biosynthesis. This is a relatively simple screen looking for compounds that enhance the survival of cells to the cytotoxic effect of the P12/UV protocol due to their ability to inhibit phospholipid biosynthesis. We used the ZR-82 strain for the screening because it is a peroxisome-deficient variant of the wild-type CHO−K1 cell line [19]. Since the peroxisomal

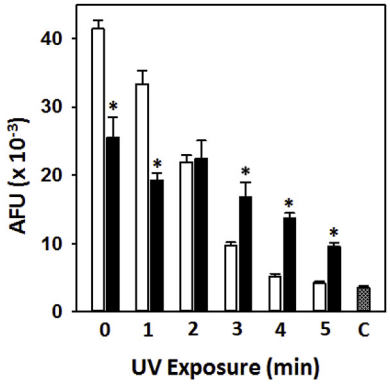


**Fig. 2. Phospholipid biosynthesis-deficient GroD1 is more resistant to the cytotoxic effects of P12/UV.** Cells were plated into a 96-well plate at $2.5 \times 10^4$ cells/well. After overnight attachment cells were treated with P12, and then irradiated for various times from underneath. Cell viability was determined using CellTiter-Blue® the following day. Values represent the average ± SD of three independent wells. White bars = ZR-82; black bars = Gro-D1. C = no cell controls. AFU (arbitrary fluorescence units). (*) indicates that the value obtained for GroD1 is significantly different ($P < 0.05$) from that obtained from ZR-82.

β-oxidation system has been shown to be important for the breakdown of pyrene-labeled fatty acids [24], we felt that this aspect of fatty acid metabolism, as a possible complicating factor, could be eliminated using this cell line. As a positive control, we used GroD1 cells. A 384-well test plate using a 4 min UV exposure resulted in a significantly elevated signal ($P < 0.01$) from wells containing GroD1 cells ($22.51 \times 10^3$ AFU, n = 96) over those containing ZR-82 cells ($12.39 \times 10^3$ AFU, n = 96).

We screened a small molecule library consisting of 1280 biologically active compounds (LOPAC; Aldrich/SIGMA). A 10 μM concentration was used for each compound and they were present only during the 3 h exposure of cells to P12. Thirty compounds showing a positive signal were rescreened for their ability to rescue ZR-82 cells and five were found to show protection consistently. Of these candidates, AG879 [25] inhibited the incorporation of $^{32}P_i$ and [methyl-$^{14}$C]choline into phospholipids (Fig. 3A). AG879 inhibited phospholipid biosynthesis by 80–90% at 10 μM with an $IC_{50}$ of 1–3 μM (Fig. 3B). AG879 had a minor effect on ATP levels over the 3 h exposure causing a 16% decrease (5.0 ± 0.2 vs. 4.2 ± 0.5 pmoles/well; $p < 0.05$), but certainly not enough to account for the dramatic decrease in phospholipid biosynthesis. Also, cell morphology was unaffected during this 3 h exposure (not shown).

Examination of individual phospholipid head group classes revealed that the biosynthesis of every head group class was affected, including cardiolipin (CL) and phosphatidylinositol (PI) (Fig. 4). At 10 μM, AG879 also inhibited phospholipid biosynthesis in other cell lines with varying effectiveness (Fig. 5); HeLa and HUH7 cells were the most affected (65–70% inhibition) while Vero and MDCK cells were less affected (40–50% inhibition).

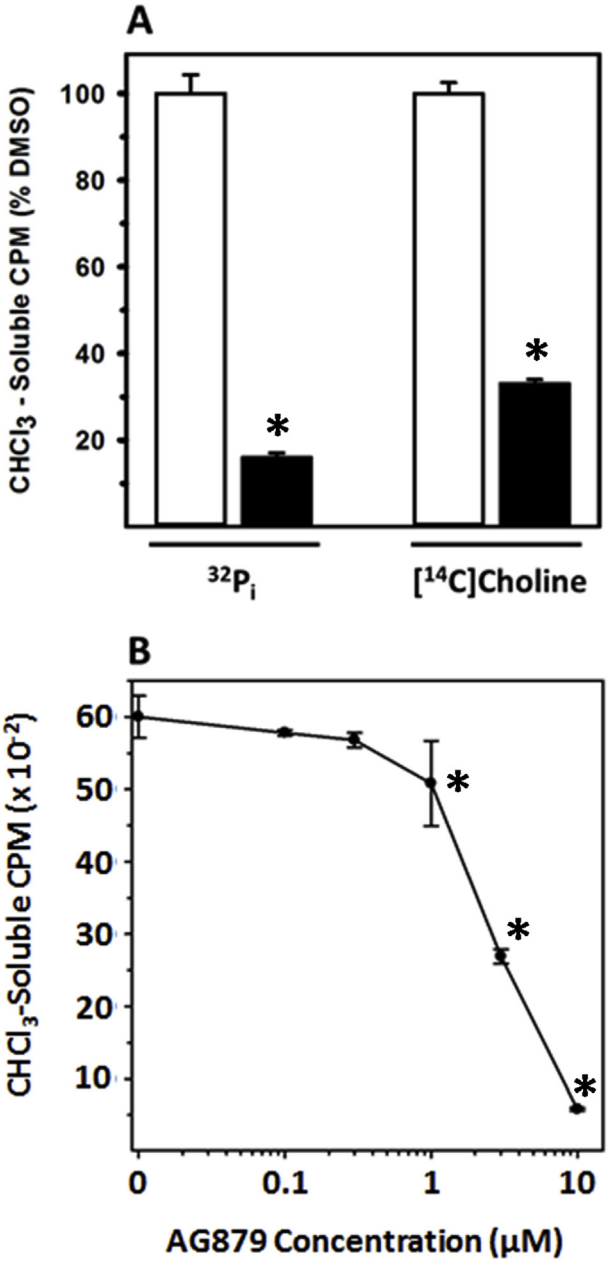


**Fig. 3. AG879 inhibits phospholipid biosynthesis in ZR-82 cells. A** - Cells were labeled with $^{32}P_i$ or [methyl-$^{14}$C]choline for 3 h in the presence of 0.1% DMSO (white bars) or 10 μM AG879 (black bars). Cellular lipids were extracted and $CHCl_3$-soluble radioactivity was determined as described in section 2.4. All values represent the averages ± SD of three separate samples. **B** - Cells were labeled with $^{32}P_i$ for 3 h in the presence of the indicated concentrations of AG879. Cellular lipids were extracted and $CHCl_3$-soluble radioactivity was quantified as described in section 2.4. Values represent the average ± range of two independent samples. **(*)** indicates that the value obtained for AG879-treated cells is significantly different ($P < 0.05$) from that obtained from DMSO-treated controls.

### *3.2. Effect of AG879 on the uptake of exogenous fatty acids into complex lipids*

AG879 inhibited the uptake of P12 into cells (Fig. 6). After subtraction of the background fluorescence as the result of RIPA buffer, at 10 μM and 30 μM AG879, P12 uptake by ZR-82 cells was reduced by approximately 45–55%. The effect of AG879 on the uptake of palmitic acid into complex lipids was also examined. Uptake of this fatty acid into phospholipids was reduced by 26% (Fig. 7A). This reduction in palmitic acid uptake into phospholipids was compensated for by an increased uptake of this fatty acid into triglycerides. Cells were grown in normal growth medium or in growth medium supplemented with 200 μM oleate (to stimulate triglyceride biosynthesis), and AG879 had no obvious effect on cellular triglyceride levels, supporting the notion that triglyceride biosynthesis and accumulation are unaffected by this compound (Fig. 7B).

### *3.3. AG879 is cytostatic*

AG879, at the concentration that inhibits phospholipid biosynthesis

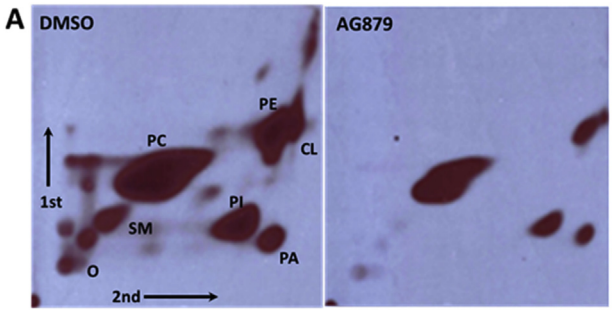


B

| | $^{32}$P Incorporation (cpm) | | |
|---|---|---|---|
| | DMSO | AG879 | AG879 (% DMSO) |
| Sphingomyelin | 476 ± 59 | 41 ± 16 | 9 |
| Phosphatidylcholine | 35414 ± 373 | 4217 ± 75 | 12 |
| Phosphatidic Acid | 2065 ± 69 | 586 ± 20 | 28 |
| Phosphatidylinositol | 5600 ± 638 | 488 ± 78 | 9 |
| Phosphatidylethanolamine | 9158 ± 261 | 2232 ± 83 | 24 |
| Cardiolipin | 1167 ± 119 | 155 ± 21 | 13 |

**Fig. 4. AG879 inhibits the synthesis of all headgroup classes in CHO cells.** **A** - Cells were labeled with $^{32}P_i$ for 3 h in the presence of 0.1% DMSO or 10 μM AG879. Cellular lipids were extracted and separated using 2D-TLC as described in section 2.4. Arrows indicate the directions of the 1st and 2nd dimension of separation. **B** - Bands of interest were scraped from the TLC plate, and the radioactivity was quantified using scintillation spectrometry. All values represent the average ± SD of three independent samples. All values obtained from AG879-treated cells displayed a $p < 0.05$ when compared to those of DMSO controls. Abbreviations: PC, phosphatidylcholine; PE, phosphatidylethanolamine; PI, phosphatidylinositol; PA, phosphatidic acid; CL, cardiolipin; SM, sphingomyelin; O, origin.

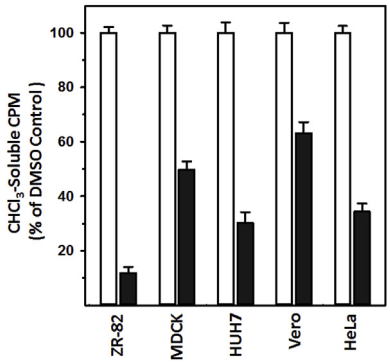


**Fig. 5. AG879 inhibits phospholipid biosynthesis in other cell lines.** Cells were labeled with $^{32}P_i$ for 3 h in the presence of 0.1% DMSO (vehicle, white bars) or 10 μM AG879 (black bars). Cellular lipids were extracted and $CHCl_3$-soluble radioactivity was determined as described in section 2.4. All values represent the average ± SD of three samples. All values obtained for AG879-treated cells is significantly different ($P < 0.05$) from DMSO-treated controls.

by 85–90%, was not cytotoxic, but rather had a cytostatic effect. ZR-82 cells in AG879-supplemented medium failed to grow and divide properly, but they maintained normal morphology (Fig. 8A and B). Cells stayed viable for at least 4 days in the presence of AG879 and were able to grow and form colonies once the inhibitor was removed (Fig. 8C). This is identical to the cytostatic behavior we have observed in the phospholipid biosynthesis-deficient mutant CHO strain, GroD1; these cells cease division when placed at the non-permissive temperature, 40°C, yet they recover growth capability and display 100% survival when returned to the permissive temperature, 33°C (data not shown).

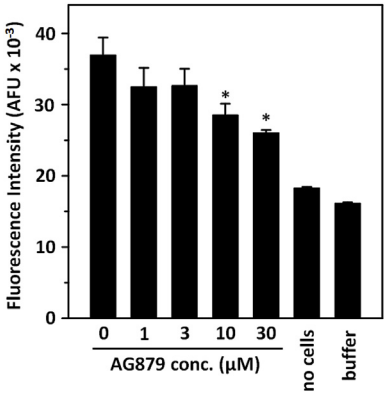


**Fig. 6. AG879 inhibits accumulation of P12.** ZR-82 cells were incubated in medium containing 20 μM P12 for 3 h, followed by a 30 min incubation in P12-free medium. Fluorescence was measured following addition of RIPA buffer to the wells as described in section 2.6. All values represent the average ± SD of four separate samples. (*) Values obtained from AG879 displayed a $p < 0.05$ when compared to those of DMSO controls.

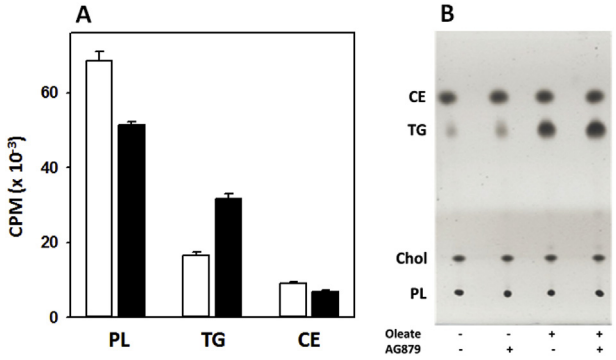


**Fig. 7. AG879 does not inhibit triglyceride or cholesterol ester biosynthesis. Panel A** - ZR-82 cells were labeled for 3 h with [9,10-$^3$H]palmitate (20 μM) and radioactivity associated with each lipid class was quantitated as described in section 2.6. All values represent the average ± SD of three separate samples. All values obtained from AG879-treated cells (black bars) displayed a $p < 0.05$ when compared to those of DMSO controls (white bars). **Panel B** – ZR-82 cells were plated out at $2 \times 10^6$ cells/100 mm diameter dish and allowed to attach overnight. Medium was replaced with medium ± 10 μM AG879 and ± 200 μM oleate. After 24 h cells were harvested with trypsin, counted and the cellular lipids were extracted as described in Materials & Methods. Lipids corresponding to $2 \times 10^6$ cells were separated on silica gel G plates. Individual lipid classes were visualized by charring.

### 3.4. AG879 inhibits fatty acid biosynthesis

We labeled the cellular lipids with [$^3$H]acetate to determine the effects of AG879 on fatty acid biosynthesis. At 10 μM, AG879 inhibited fatty acid biosynthesis by approximately 90% (Fig. 9). This inhibition was similar to the well-established fatty acid synthase inhibitor, cerulenin [26]. Our data show that, as expected, cerulenin also inhibited phospholipid biosynthesis, but it had much less of an effect than AG879, demonstrating only a 25% inhibition at 30 μM (Fig. 9). We cannot rule out the possibility that AG879 affects radioactive acetate uptake or activation versus direct inhibition of *de novo* fatty acid synthesis.

### 3.5. Fatty acid supplementation partially recovers phospholipid synthesis in the presence of AG879

If inhibition of *de novo* fatty acid biosynthesis is the primary target of AG879 we may be able to reverse AG879-mediated phospholipid biosynthesis inhibition by supplementation of the medium with

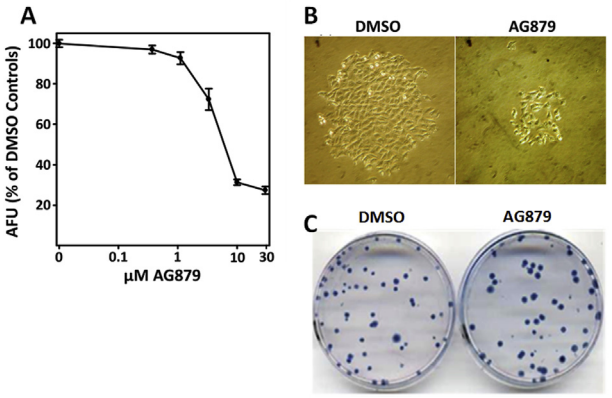


**Fig. 8. AG879 inhibits cell growth, but is not cytotoxic. Panel A** – ZR-82 cells were plated into 12-well dishes at $2.5 \times 10^5$ cells/well. Following overnight attachment AG879 was added and cells were allowed to grow for 48 h @ 37°C before cell density/survival was measured using CellTiter-Blue. All values represent the average ± SD of 6 wells. All values obtained from AG879-treated cells (other than 0.3 μM AG879) displayed a significant difference ($P < 0.05$) from the value obtained from untreated control cells. **Panel B -** ZR-82 cells were plated into 60 mm diameter dishes at low density (100 cells/dish) and allowed to attach overnight. AG879 (10 μM) or DMSO (0.1%) was added the next day. After 6 days, colonies were located and photographed at 100X using a Leitz phase contrast microscope. **Panel C-** ZR-82 cells were plated into 60 mm diameter dishes at low density (100 cells/dish) and allowed to attach overnight. AG879 (10 μM) or DMSO (0.1%) was added the next day. DMSO-treated cells were allowed to grow for 10 days prior to staining with Coomassie blue. AG879-treated cells were maintained in the presence of the compound for 4 days, medium was then change to AG879-free medium and colonies resulting from surviving cells were stained after an additional 10 days of growth.

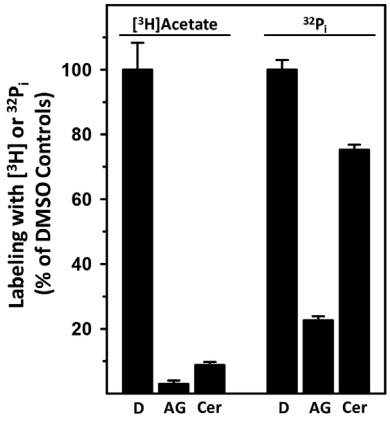


**Fig. 9. AG879 and cerulenin inhibit fatty acid and phospholipid biosynthesis in ZR-82 cells. Fatty acid labeling:** Cells were labeled with [$^3$H] acetate for 3 h in the presence of 0.1% DMSO (D), 10 μM AG879 (AG) or 30 μM cerulenin (Cer). Fatty acid synthesis was determined as described in section 2.5. **Phospholipid labeling:** Cells were labeled with $^{32}P_i$ for 3 h in the presence of 0.1% DMSO, 10 μM AG879 (AG) or 30 μM cerulenin (Cer) and phospholipid production was determined as described in section 2.4. All values represent the average ± SD of three separate samples. All values obtained from AG879-treated and cerulenin-treated cells displayed a $p < 0.05$ when compared to those of DMSO controls.

exogenous fatty acid. Supplementing the labeling medium with 100 μM oleic acid had a modest restoration of phospholipid biosynthesis in the presence of both AG879 and cerulenin (Fig. 10), this was far from complete. In a separate experiment, increasing the supplementation of oleate to 200 μM had little further effect (Fig. 10). Increasing the level of supplemental oleate above 200 μM resulted in cytotoxicity.

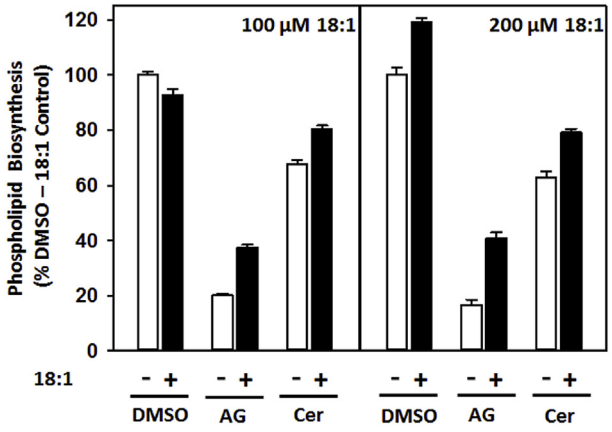


**Fig. 10. Fatty acid supplementation partially rescues phospholipid inhibition by AG879 and cerulenin.** Cells were labeled for 3 h in medium containing $^{32}P_i$ in the presence or absence of 100 μM or 200 μM oleate. Labeled lipids were extracted and $CHCl_3$-soluble radioactivity was quantitated as described in section 2.4. The data describing the effects of the two different concentrations of oleate were obtained from independently performed experiments. All values represent the average ± SD of three samples. All values obtained from cells supplemented with oleate displayed a $p < 0.05$ when compared to those of controls.

### *3.6. Comparison of inhibition of phospholipid biosynthesis by other compounds points to inhibition of both the Akt and MEK pathways by AG879*

AG879 was developed as a receptor tyrosine kinase (RTK) inhibitor and was found to inhibit the RTK growth receptors HER2 and tropomyosin analogue receptor kinase (TrkA) [27]. We examined phospholipid biosynthesis in the presence of other RTK inhibitors using concentrations that have been shown to be effective in other cell culture systems (Fig. 11). Tyrphostin AG1478, which has been shown to inhibit the epidermal growth factor receptor (EGFR; ref 27), also inhibits phospholipid biosynthesis although not as effectively as AG879 at the concentration used (20 μM). Afatanib, a HER2/EGFR inhibitor which acts by covalently modifying a crucial cysteine residue within the receptor [28], had little effect at 1 μM. GW441756, another inhibitor of TrkA [29], had only a minimal effect on phospholipid biosynthesis at

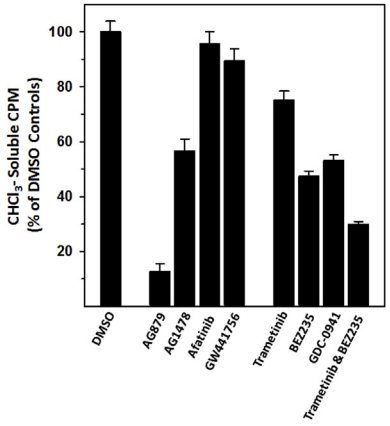


**Fig. 11. Inhibition of phospholipid biosynthesis targeting rtk and rtk-dependent pathways**. Cells were labeled with $^{32}P_i$ for 3 h in the presence of each compound. Cellular lipids were extracted and $CHCl_3$-soluble radioactivity was determined as described in Material & Methods. AG879 (10 μM), AG1478 (20 μM), afatinib (1 μM), GW441756 (2 μM), trametinib (10 μM), BEZ235 (2 μM), GDC-0941 (3 μM). All values represent the average ± SD of three separate samples. All values obtained from compounds, other than afatinib, displayed a $p < 0.05$ when compared to those of DMSO controls.

2 μM.

We also examined inhibitors of elements involved in the signaling pathways known to be activated by RTK's, including the MEK and Akt pathways [30]. Trametinib, an inhibitor of MEK [31], caused a 25% decrease in phospholipid labeling, while BEZ235 and GDC-0941, both inhibitors of the Akt pathway [32–34], caused a 45–50% inhibition (Fig. 11). The addition of BEZ235 and trametinib together had an additive effect, resulting in a 70–75% reduction in phospholipid labeling, closer to the values obtained using AG879.

## 4. Discussion

From a small molecule library of 1280 compounds we have identified a compound, AG879, which inhibits phospholipid biosynthesis. Our screen has the advantage that it quantifies the ability of a compound to allow cells to survive the P12/UV protocol. As a result, candidate compounds are not cytotoxic, at least in the short-term. This eliminates a common cause for false positives. We identified relatively few candidates from the library (five), reducing our need for the more time consuming orthogonal assays. From the LOPAC library, AG879 was the only compound found to be effective in reducing phospholipid biosynthesis in ZR-82 cells, displaying an $IC_{50}$ of 1–3 μM in the presence of 10% serum. We show here that AG879 is an extremely effective inhibitor of phospholipid biosynthesis, inhibiting phospholipid biosynthesis by 80–90%.

One might expect that decreasing phospholipid biosynthesis by 80–90% would more severely reduce incorporation of fatty acid into these lipids. However, the decrease in fatty acid uptake into the phospholipids of AG879-treated ZR-82 cells was only moderately reduced. This may be explained by the fact that the fatty acid composition of pre-existing phospholipids are constantly being modified through the Lands Cycle [35] and this form of fatty acid incorporation, in the short-term, should be relatively unaffected by inhibition of *de novo* phospholipid biosynthesis. This suggests that the Land's cycle is an important process for the uptake of exogenous fatty acids into phospholipid pools. Similar results were observed in the phospholipid biosynthesis-deficient GroD1 cell line [20].

While it is beyond the scope of this study, we can speculate a bit on the possible mechanism behind AG879's inhibition of phospholipid biosynthesis. First, we do not think that phosphatidate phosphohydrolase (lipin 1) is a target for AG879. The GroD1 cell line, displaying greatly reduced levels of this activity, displays severely limited phospholipid biosynthesis, phosphatidylcholine and phosphatidylethanolamine biosynthesis, while phosphatidylinositol synthesis is not affected and phosphatidic acid accumulates [20]. Also, triacylglycerol biosynthesis is greatly reduced in GroD1 cells. These data fit well with the demonstrated decrease in phosphatidate phosphohydrolase activity in these cells; phosphatidylcholine, phosphatidylethanolamine and triacylglycerol biosynthesis are all dependent on this activity, while synthesis of phosphatidylinositol and phosphatidic acid are not. The data obtained after addition of AG879 to ZR-82 cells are significantly different. Addition of AG879 resulted in reduced $^{32}P_i$ labeling of all head group classes. Also, the ability to synthesize or accumulate triacylglycerols (TG) was unaffected by AG879; this ruled out phosphatidate phosphohydrolase as a primary target. Also, the facts that AG879-treated cells were capable of normal incorporation of fatty acids into trigycerides argue that early steps shared by triglyceride and phospholipid biosynthesis, such as glycerol-3-phosphate O-acyltransferase and 1-acylglycerol-3-phosphate O-acyltransferase [20] are unaffected by AG879.

It may be that fatty acid biosynthesis is the primary target of AG879, with phospholipid biosynthesis being a downstream target, heavily dependent on *de novo* fatty acid biosynthesis; inhibition of phospholipid biosynthesis by inhibition of FAS has previously been demonstrated in bacterial and animal cell systems [36,37]. Developed as an inhibitor of RTK's [27], AG879 has been shown to inhibit the HER2 receptor as well as other growth factor receptors which stimulate lipid biosynthesis [38,39] and activation of the HER2 receptor results in the activation of fatty acid synthase (FAS) through phosphorylation of a tyrosine residue [40]. CHO cells do express the HER2 receptor, although minimally [41], and appear to depend more on the insulin receptor for cell growth [42]; both the HER2 and insulin receptors are RTK's. Inhibition of elements in the two signaling pathways known to be activated by RTK's, the Akt and MEK dependent pathways, resulted in inhibition of phospholipid biosynthesis (Fig. 11).

A possible argument against fatty acid synthase as the sole target of AG879 in phospholipid biosynthesis comes from the fact that cerulenin, a well-established inhibitor of fatty acid synthase [26,43], resulted in inhibition of fatty acid biosynthesis to a similar degree as AG879, but was less effective in inhibiting phospholipid biosynthesis. Also, supplementation of medium with exogenous fatty acid only partially restored phospholipid biosynthesis (Fig. 10).

Both fatty acid biosynthesis and phospholipid biosynthesis have been proposed as targets for antiviral and anticancer therapy [1,10,14,44]. AG879 was initially developed as an anticancer reagent and has been shown to have anticancer activity in *in vitro* model systems [45,46]. AG879 was also shown to be an effective antiviral [47,48], inhibiting the replication of influenza virus as well as other viruses in cultured cell systems and rescuing mice from lethal challenges of influenza virus [47]. Inhibition of phospholipid biosynthesis is not cytotoxic in the short-term in culture. CHO cells tolerated AG879 for at least four days and isolation of phospholipid biosynthesis mutants commonly subject the candidate mutants to at least 24 h under non-permissive conditions, yet they survive and continue to divide upon return to permissive conditions [3–6]. Also, mice tolerated AG879 quite well over a period of 7 days [47]. This makes phospholipid/fatty acid biosynthesis inhibitors attractive treatments of short-term pathologies such as influenza infection since such treatment may be well tolerated. While this evidence is compelling, AG879 has been shown to inhibit other cell processes [49] so it is not yet possible to say that its antiviral properties are a direct result of its inhibition of host fatty acid or phospholipid biosynthesis.

In summary, the major findings of this work include: 1 – development of a cell-based, high-throughput screening protocol that is capable of identifying an inhibitor of phospholipid biosynthesis from a small molecule library; 2 – identification of a new, potent inhibitor of animal cell phospholipid biosynthesis, AG879 that has been previously shown to inhibit antiviral replication; 3- evidence, using AG879, that *de novo* fatty acid biosynthesis may be important for phospholipid biosynthesis in animal cells; 4 – evidence, using AG879 and other inhibitors, that the RTK receptor-dependent pathways are important for animal cell phospholipid biosynthesis.

Further studies with additional libraries are expected to yield novel phospholipid biosynthesis inhibitors. Such compounds will be useful in establishing, or discrediting phospholipid biosynthesis inhibition as a viable approach to anticancer or antiviral therapies. Additional inhibitors of phospholipid biosynthesis can also be utilized to identify factors which are important for their synthesis.

## Acknowledgements

We thank Dr. Esther Bullitt for critical evaluation of the manuscript. This work was supported by the grants from the NIH: R01 GM107675, P03DK046200, and 1UL1TR001430.

## References

[1] M. Cheng, Z.M. Bhujwalla, K. Glunde, Targeting phospholipid metabolism in cancer, Front. Oncol. 6 (2016) 266.
[2] C. Huang, C. Freter, Lipid metabolism, apoptosis and cancer therapy, Int. J. Mol. Sci. 16 (2015) 924–949.
[3] J.D. Esko, C.R.H. Raetz, Autoradiographic detection of animal cell membrane mutants altered in phosphatidylcholine synthesis, Proc. Natl. Acad. Sci. U.S.A. 77

(1980) 5192–5196.
[4] J.D. Esko, M. Nishijima, C.R.H. Raetz, Animal cells dependent on exogenous phosphatidylcholine for membrane biogenesis, Proc. Natl. Acad. Sci. U.S.A. 79 (1982) 1698–1702.
[5] M.A. Miller, C. Kent, Characterization of the pathways for phosphatidylethanolamine biosynthesis in Chinese hamster ovary mutant and parental cell lines, J. Biol. Chem. 261 (1986) 9753–9761.
[6] O. Kuge, M. Nishijima, Y. Akamatsu, Isolation of a somatic-cell mutant defective in phosphatidylserine biosynthesis, Proc. Natl. Acad. Sci. U.S.A. 82 (1985) 1926–1930.
[7] S. Trousil, M. Kaliszczak, Z. Schug, Q.D. Nguyen, G. Tomasi, R. Favicchio, D. Brickute, R. Fortt, F.J. Twyman, L. Carroll, A. Kalusa, N. Navaratnam, T. Adejumo, D. Carling, E. Gottlieb, E.O. Aboagye, The novel choline kinase inhibitor ICL-CCIC-0019 reprograms cellular metabolism and inhibits cancer cell growth, Oncotarget 7 (2016) 37103–37120.
[8] J.M. Mazarico, V.J. Sánchez-Arévalo Lobo, R. Favicchio, W. Greenhalf, E. Costello, E. Carrillo-de Santa Pau, M. Marqués, J.C. Lacal, E. Aboagye, F.X. Real, Choline kinase alpha (CHKα) as a therapeutic target in pancreatic ductal adenocarcinoma: expression, predictive value, and sensitivity to inhibitors, Mol. Canc. Therapeut. 15 (2016) 323–333.
[9] L. Fuentes, R. Pérez, M.L. Nieto, J. Balsinde, M.A. Balboa, Bromoenol lactone promotes cell death by a mechanism involving phosphatidate phosphohydrolase-1 rather than calcium-independent phospholipase A2, J. Biol. Chem. 278 (2003) 44683–44690.
[10] R. Guinea, L. Carrasco, Phospholipid biosynthesis and poliovirus genome replication, two coupled phenomena, EMBO J. 9 (1990) 2011–2016.
[11] D.E. Vance, E.M. Trip, H.B. Paddon, Poliovirus increases phosphatidylcholine biosynthesis in HeLa cells by stimulation of the rate-limiting reaction catalyzed by CTP: phosphocholine cytidylyltransferase, J. Biol. Chem. 255 (1980) 1064–1069.
[12] G.A. Belov, E. Sztul, Rewiring of cellular membrane homeostasis by picornaviruses, J. Virol. 88 (2014) 9478–9489.
[13] J. Zhang, Z. Zhang, V. Chukkapalli, J.A. Nchoutmboube, J. Li, G. Randall, G.A. Belov, X. Wang, Positive-strand RNA viruses stimulate host phosphatidylcholine synthesis at viral replication sites, Proc. Natl. Acad. Sci. U.S.A. 113 (2016) 1064–1073 PMID: 26858414.
[14] M. Sharma, Z. Sasvari, P.D. Nagy, Inhibition of phospholipid biosynthesis decreases the activity of the tombusvirus replicase and alters the subcellular localization of replication proteins, Virology 415 (2011) 141–152.
[15] J.,. Balsinde, E.A. Dennis, Bromoenol lactone inhibits magnesium-dependent phosphatidate phosphohydrolase and blocks triacylglycerol biosynthesis in mouse P388D1 macrophages, J. Biol. Chem. 271 (1996) 31937–31941.
[16] E.J. Ackermann, K. Conde-Frieboes, E.A. Dennis, Inhibition of macrophage Ca(2+)-independent phospholipase A2 by bromoenol lactone and trifluoromethyl ketones, J. Biol. Chem. 270 (1995) 445–450.
[17] S.G. Zech, A. Kohlmann, T. Zhou, F. Li, R.M. Squillace, L.E. Parillon, M.T. Greenfield, D.P. Miller, J. Qi, R.M. Thomas, Y. Wang, Y. Xu, J.J. Miret, W.C. Shakespeare, X. Zhu, D.C. Dalgarno, Novel small molecule inhibitors of choline kinase identified by fragment-based drug discovery, J. Med. Chem. 59 (2016) 671–686.
[18] A. Estévez-Braun, A.G. Ravelo, E. Pérez-Sacau, J.C. Lacal, A new family of choline kinase inhibitors with antiproliferative and antitumor activity derived from natural products, Clin. Transl. Oncol. 17 (2015) 74–84.
[19] R.A. Zoeller, C.R.H. Raetz, Isolation of animal cell mutants deficient in plasmalogen biosynthesis and peroxisome assembly, Proc. Natl. Acad. Sci. U.S.A. 83 (1986) 5170–5174.
[20] J.F. Haller, C. Smith, D. Liu, H. Zheng, K. Tornheim, G. S Han, G.M. Carman, R.A. Zoeller, Isolation of novel animal cell lines defective in glycerolipid biosynthesis reveals mutations in glucose-6-phosphate isomerase, J. Biol. Chem. 285 (2010) 866–877.
[21] E.G. Bligh, W.J. Dyer, A rapid method of total lipid extraction and purification, Can. J. Biochem. Physiol. 37 (1959) 911–917.
[22] G. Palumbo, F. Zullo, The use of iodine staining for the quantitative analysis of lipids separated by thin layer chromatography, Lipids 22 (1987) 201–205.
[23] X. Tang, M.G. Benesch, D.N. Brindley, Lipid phosphate phosphatases and their roles in mammalian physiology and pathology, J. Lipid Res. 56 (2015) 2048–2060.
[24] S. Gatt, J. Bremer, H. Osmundsen, Pyrene dodecanoic acid coenzyme A ester: peroxisomal oxidation and chain shortening, Biochim. Biophys. Acta 958 (1988) 130–133.
[25] M. Ohmichi, L. Pang, V. Ribon, A. Gazit, A. Levitzki, A.R. Saltiel, The tyrosine kinase inhibitor tyrphostin blocks the cellular actions of nerve growth factor, Biochemistry 32 (1993) 4650–4658.
[26] R. Flavin, S. Peluso, P.L. Nguyen, M. Loda, Fatty acid synthase as a potential therapeutic target in cancer, Future Oncol. 6 (2010) 551–562.
[27] A. Levitzki, A. Gazit, Tyrosine kinase inhibition: an approach to drug development, Science 267 (1995) 1782–1788.
[28] D. Li, L. Ambrogio, T. Shimamura, S. Kubo, M. Takahashi, L.R. Chirieac, R.F. Padera, G.I. Shapiro, A. Baum, F. Himmelsbach, W.J. Rettig, M. Meyerson, F. Solca, H. Greulich, K.K. Wong, BIBW2992, an irreversible EGFR/HER2 inhibitor highly effective in preclinical lung cancer models, Oncogene 27 (2008) 4702–4711.
[29] E.R. Wood, L. Kuype, K.G. Petrov, R.N. Hunter 3rd, P.A. Harris, K. Lackey, Discovery and in vitro evaluation of potent TrkA kinase inhibitors: oxindole and aza-oxindoles, Bioorg. Med. Chem. Lett 14 (2004) 953–957.
[30] W. Zheng, A. Aspelund, K. Alitalo, Lymphangiogenic factors, mechanisms, and applications, J. Clin. Invest. 124 (2014) 878–887.
[31] I. Lugowska, H. Koseła-Paterczyk, K. Kozak, P. Rutkowski, Trametinib: a MEK inhibitor for management of metastatic melanoma, OncoTargets Ther. 8 (2015) 2251–2259.
[32] H.Y. Zhou, S.L. Huang, Current development of the second generation of mTOR inhibitors as anticancer agents, Chin. J. Canc. 31 (2012) 8–18.
[33] A.J. Folkes, K. Ahmadi, W.K. Alderton, S. Alix, S.J. Baker, G. Box, I.S. Chuckowree, P.A. Clarke, P. Depledge, S.A. Eccles, L.S. Friedman, A. Hayes, T.C. Hancox, A. Kugendradas, L. Lensun, P. Moore, A.G. Olivero, J. Pang, S. Patel, G.H. Pergl-Wilson, F.I. Raynaud, A. Robson, N. Saghir, L. Salphati, S. Sohal, M.H. Ultsch, M. Valenti, H.J.A. Wallweber, N.C. Wan, C. Wiesmann, P. Workman, A. Zhyvoloup, M.J. Zvelebil, S.J. Shuttleworth, The identification of 2-(1H-indazol-4-yl)-6-(4-methanesulfonyl-piperazin-1-ylmethyl)-4-morpholin-4-yl-thieno[3,2-d]pyrimidine (GDC-0941) as a potent, selective, orally bioavailable inhibitor of class I PI3 kinase for the treatment of cancer, J. Med. Chem. 51 (2008) 5522–5532.
[34] T.T. Junttila, R.W. Akita, K. Parsons, C. Fields, G.D. Lewis Phillips, L.S. Friedman, D. Sampath, M.X. Sliwkowski, Ligand-independent HER2/HER3/PI3K complex is disrupted by trastuzumab and is effectively inhibited by the PI3K inhibitor GDC-0941, Cancer Cell 15 (2009) 429–440.
[35] H. Shindou, T. Shimizu, Acyl-CoA:lysophospholipid acyltransferases, J. Biol. Chem. 284 (2009) 1–5.
[36] L. Mao, K. Inoue, Y. Tao, G.T. Montelione, A.E. McDermott, M. Inouye, Suppression of phospholipid biosynthesis by cerulenin in the condensed Single-Protein-Production (cSPP) system, J. Biomol. NMR 49 (2011) 131–137.
[37] J. Ross, A.M. Najjar, M. Sankaranarayanapillai, W.P. Tong, K. Kaluarachchi, S.M. Ronen, Fatty acid synthase inhibition results in a magnetic resonance–detectable drop in phosphocholine, Mol. Canc. Therapeut. 7 (2008) 2556–2565.
[38] J. Baumann, C. Sevinsky, D.S. Conklin, Lipid biology of breast cancer, Biochim. Biophys. Acta 1831 (2013) 1509–1517.
[39] M.P. Czech, M. Tencerova, D.J. Pedersen, M. Aouadi, Insulin signalling mechanisms for triacylglycerol storage, Diabetologia 56 (2013) 949–964.
[40] Q. Jin, L.X. Yuan, D. Boulbes, J.M. Baek, Y.N. Wang, D. Gomez-Cabello, D.H. Hawke, S.C. Yeung, M.H. Lee, G.N. Hortobagy, M.C. Hung, F.J. Esteva, Fatty acid synthase phosphorylation: a novel therapeutic target in HER2-overexpressing breast cancer cells, Breast Cancer Res. 12 (2010) R96.
[41] A.H. Colagar, O. Amjadi, R. Valadan, A. Rafiei, Minimal HER1 and HER2 expressions in CHO and HEK-293 cells cause them appropriate negative cells for HERs-related studies, Res.Mol. Med. 1 (2013) 6–12.
[42] M. Mamounas, D. Gervin, E. Englesberg, The insulin receptor as a transmitter of a mitogenic signal in Chinese hamster ovary CHO-K1 cells, Proc. Natl. Acad. Sci. U.S.A. 86 (1989) 9294–9298.
[43] H. Funabashi, A. Kawaguchi, H. Tomoda, S. Omura, S. Okuda, S. Iwasaki, Binding site of ceruleniin in fatty acid synthetase, J. Biochem. 105 (1989) 751–755.
[44] E. Currie, A. Schulze, R. Zechner, T.C. Walther, R.V. Farese Jr., Cellular fatty acid metabolism and cancer, Cell Metabol. 18 (2013) 153–161.
[45] M. Rende, A. Pistilli, A.M. Stabile, A. Terenzi, A. Cattaneo, G. Ugolini, P. Sanna, Role of nerve growth factor and its receptors in non-nervous cancer growth: efficacy of a tyrosine kinase inhibitor (AG879) and neutralizing antibodies antityrosine kinase receptor A and antinerve growth factor: an in-vitro and in-vivo study, Anti Canccer Drugs 17 (2008) 929–941.
[46] T.W. Grunt, Tyrphostins and retinoids cooperate during inhibition of in vitro growth of ovarian cancer cells, Cancer Lett. 189 (2003) 147–156.
[47] N. Kumar, N.R. Sharma, H. Ly, T.G. Parslow, Y. Liang, Receptor tyrosine kinase inhibitors that block replication of influenza a and other viruses, Antimicrob. Agents Chemother. 55 (2011) 5553–5559.
[48] N. Kumar, Y. Liang, T.G. Parslow, Y. Liang, Receptor tyrosine kinase inhibitors block multiple steps of influenza a virus replication, J. Virol. 85 (2011) 2818–2827.
[49] H. Yu, B. Zou, X. Wang, M. Li, Effect of tyrphostin AG879 on Kv 4.2 and Kv 4.3 potassium channels, Br. J. Pharmacol. 172 (2015) 3370–3382.